




## ORIGINAL ARTICLE

# The cyclic motor patterns in the human colon

Maham Pervez<sup>1</sup>  | Elyanne Ratcliffe<sup>2</sup> | Sean P. Parsons<sup>1</sup> | Ji-Hong Chen<sup>1</sup>  | Jan D. Huizinga<sup>1</sup> 

<sup>1</sup>Department of Medicine, Division of Gastroenterology, Farncombe Family Digestive Health Research Institute, McMaster University, Hamilton, ON, Canada

<sup>2</sup>Department of Pediatrics, McMaster University, Hamilton, ON, Canada

## Correspondence

Ji-Hong Chen, Department of Medicine, Division of Gastroenterology, Farncombe Family Digestive Health Research Institute, McMaster University, HSC-3H1F, 1200 Main Street West, Hamilton L8N 3Z5, ON, Canada.  
Email: chen338@mcmaster.ca

## Funding information

Canadian Institutes of Health Research; Institute of Nutrition, Metabolism and Diabetes; Hamilton Academic Health Sciences Organization; Farncombe Family Digestive Health Research Institute; Canadian Foundation for Innovation

## Abstract

**Background:** High-resolution colonic manometry gives an unprecedented window into motor patterns of the human colon. Our objective was to characterize motor activities throughout the entire colon that possessed persistent rhythmicity and spanning at least 5 cm.

**Methods:** High-resolution colonic manometry using an 84-channel water-perfused catheter was performed in 19 healthy volunteers. Rhythmic activity was assessed during baseline, proximal balloon distention, meal, and bisacodyl administration.

**Key Results:** Throughout the entire colon, a cyclic motor pattern occurred either in isolation or following a high-amplitude propagating pressure wave (HAPW), consisting of clusters of pressure waves at a frequency centered on 11–13 cycles/min, unrelated to breathing. The cluster duration was 1–6 minutes; the pressure waves traveled for 8–27 cm, lasting 5–8 seconds. The clusters themselves could be rhythmic at 0.5–2 cpm. The propagation direction of the individual pressure waves was mixed with >50% occurring simultaneously. This high-frequency cyclic motor pattern co-existed with the well-known low-frequency cyclic motor pattern centered on 3–4 cpm. In the rectum, the low-frequency cyclic motor pattern dominated, propagating predominantly in retrograde direction. Proximal balloon distention, a meal and bisacodyl administration induced HAPWs followed by cyclic motor patterns.

**Conclusions and Inferences:** Within cyclic motor patterns, retrograde propagating, low-frequency pressure waves dominate in the rectum, likely keeping the rectum empty; and mixed propagation, high-frequency pressure waves dominate in the colon, likely promoting absorption and storage, hence contributing to continence. Propagation and frequency characteristics are likely determined by network properties of the interstitial cells of Cajal.

## KEYWORDS

colonic motility, cyclic motor pattern, high-resolution colonic manometry, interstitial cells of Cajal, rectal pressure waves

**Abbreviations:** CMP, Cyclic motor pattern; HAPW, High-amplitude propagating pressure wave; SPW, Simultaneous pressure wave.

Jan D. Huizinga and Ji-Hong Chen are co-senior authors.

## 1 | INTRODUCTION

Colonic manometry is the method of choice to diagnose potential colonic motor disorders and the procedure is recommended by consensus guidelines.<sup>1,2</sup> Detailed analysis of colonic motility patterns is now possible using high-resolution manometry. Studies in patients have proposed biomarkers of disease identified by high-resolution manometry.<sup>3,4</sup> However, detailed analysis of normal motor patterns in healthy subjects is still in its infancy and claims for biomarkers of disease deserve scrutiny as more features of normal motor activity become known. In adult and pediatric colonic manometry, the primary goal is to confirm or exclude colonic inertia which is assessed by the colon's ability to generate high-amplitude propagating pressure waves (abbreviated as HAPWs or HAPCs or HAPs), either spontaneously, in response to a meal or in response to bisacodyl. Based on the HAPW appearance, guidelines have been developed to distinguish normal from abnormal activity.<sup>1,2</sup> Although very useful, in particular when colonic inertia is excluded, focusing only on HAPWs assesses only a very small part of colonic motor activity. It is now clear from studies using high-resolution colonic manometry (HRCM) that other motor patterns deserve to be incorporated in the assessment of colon motility such as "simultaneous pressure waves"<sup>5-7</sup> and the "cyclic motor pattern"<sup>3,4,8</sup> or "periodic motor activity".<sup>9</sup> Dinning et al proposed that the absence of an increase in the cyclic motor pattern after a meal was a feature of slow transit constipation,<sup>4</sup> and Lindley and co-workers proposed that the occurrence of a cyclic motor pattern in between bisacodyl-induced HAPWs was a biomarker of constipation.<sup>3</sup> Hence, cyclic motor patterns deserve extensive investigation. Dinning and co-workers defined the cyclic motor pattern as repetitive propagating pressure events with a frequency of 2-6 per minutes and proposed that the pressure wave frequency and propagation characteristics were orchestrated by interstitial cells of Cajal (ICC).<sup>4</sup> Consistently, myogenic activity in the human colon has most commonly been attributed to pacemaker-generated activity ranging from 2 to 8 cpm, often very evident in the human rectum.<sup>10-13</sup> Interestingly, direct measurement of slow wave activity in the human colon also showed prominent frequencies around 12 cpm.<sup>14-16</sup>

A major reason for exploration of rhythmic motor patterns that are likely associated with ICC pacemaker activity<sup>13,17-19</sup> is the consistent finding that ICC are markedly reduced in patients with severe constipation who underwent surgery.<sup>3,20,21</sup> It is not known if loss of ICC is a primary cause of constipation but loss of ICC causes dysmotility.<sup>22,23</sup> Hence, an understanding of ICC-directed motor patterns in healthy volunteers and patients may shed light on the consequences of loss of ICC. This may contribute to our understanding of the pathophysiology of severe constipation. Research into plasticity of ICC may lead to future opportunities for restoration of function.<sup>24</sup>

Although all motor patterns of the human colon can occur in a rhythmic manner, the objective of the present study was to explore all propagating motor patterns over at least 5 cm in the colon and at least 3 cm in the rectum that have rhythmicity as a defining and constant feature.

### Key Points

- High-Resolution Colonic Manometry allows exploration of motor patterns of the human colon as pressure waves. We characterized all motor patterns with persistent intrinsic rhythmicity, using 84 sensors, 1 cm apart, throughout the entire colon.
- A prominent high-frequency cyclic motor pattern, centered around 12 cpm, was characterized that was unrelated to breathing and co-existed with the well-known cyclic motor pattern centered around 3 cpm.
- The high-frequency cyclic motor pattern occurred prominently in the wake of 44% of the high amplitude propagating pressure waves (HAPWs).

## 2 | METHODS

### 2.1 | Study subjects

Nineteen healthy subjects with an average age of  $36.4 \pm 14.0$  years (range: 19-60 years; 7 females) were recruited as volunteers through local advertising. In 17 of these volunteers, the characteristics of the simultaneous pressure waves have been analyzed and published,<sup>6</sup> but the cyclic motor patterns were not analyzed previously nor reported on. All participants gave written informed consent and all procedures were approved by the Hamilton Integrated Research Ethics Board (HiREB). Exclusion criteria included the following: abdominal surgery, hepatic, kidney or cardiac diseases, connective tissue disorders, central nervous system disorders, thyroid diseases, prostate diseases, or malignancies. All subjects had normal stool consistency and normal bowel frequency; between 1 every 3 days and 3 per day. None of the subjects experienced defecation difficulty, nor did they take any medication that might influence bowel movements.

### 2.2 | High-resolution colonic manometry

High-resolution colonic manometry (HRCM) was performed on a custom-made platform (Medical Measurement Systems (MMS); Laborie). One of two 84-sensor water-perfused catheter were used (diameter: 8.0 mm; Mui Scientific) that included either two 10-cm long balloons between sensors 10 and 11 (proximal balloon) and 40 and 41 (distal balloon), or a single balloon between sensors 10 and 11 only. No sensors were present in these 10 cm segments. In seven volunteers, a separate rectal balloon was used in place of the distal balloon. The catheter is calibrated the morning of the colonoscopy with 0 mm Hg pressure corresponding to the position of the catheter inside the patient while lying on the hospital bed. The bed is raised during the colonoscopy and lowered thereafter to the calibrated position. The catheter was inserted with minimal sedation (fentanyl iv 50-100 mcg

and midazolam iv 2-5 mg) with the assistance of a colonoscope after a bowel cleaning procedure using an inert osmotic laxative (PEG-Lyte, Pendopharm, Montreal, QC, Canada), but no use of stimulant laxatives such as bisacodyl. For the bowel cleaning procedure, 3 L of PEG (70 g/L) was taken between 4 and 6 PM the day before the procedure, with more water consumed if needed to have all solids removed. The next morning, 1 L was taken at 4 AM. The tip of the catheter was clipped to the mucosa via a fish line, a few cm distal to the cecum. The catheter was made of 100% silicon; after use, an extensive approved cleaning procedure was executed followed by sterilization. A disposable dual lumen stomach tube (3.3 mm  $\times$  91 cm; Salem Sump™, Covidien Inc) was placed in the rectum for passive liquid drainage introduced by the water perfusion system. In 18 of the 19 subjects, the drainage tube was present for the entire duration of the study. During the recording, the total diameter of the tubing (accounting the water-perfused catheter and the drainage tube) in the participant was 11 mm. This diameter is comparable to the 3D high-definition anorectal manometry (HDAM) catheters (diameter: 10.8 mm).<sup>25</sup>

### 2.3 | Protocol

A minimum of thirty minutes after the scope was withdrawn, a 90 minutes recording of baseline activity was started (Table S1). The response to a 5-min balloon distension at the proximal colon and/or the rectum was investigated. The balloon was inflated until first sensation was reported; this was followed by incremental increases in balloon volume by 60 mL until the maximum tolerated volume was achieved which was between 250 and 400 mL air. In each of these periods, the volume was sustained for a short period (between 2 and 3 minutes). The extent of the balloon inflation was determined by the subject's level of discomfort in response to the distension. Inflation was stopped when the discomfort reached 6-7 on a 10-point scale, but such that the subject could manage the balloon distension for 5 minutes. After the 5-min distension, the balloon was deflated. Analysis of the response to balloon distension was performed on the 5 minutes period of sustained distension, and a 15-min period after deflation. After the balloon distension, a meal was given (500 g of organic vanilla yogurt fortified with organic milk fat to 40% fat (Mapleton Organics)), providing 800-1000 kcal (based on the volume consumed). Its effect was observed for 90 minutes. Lastly, the effects of 10 mg of bisacodyl (Dulcolax; Boehringer Ingelheim, Sanofi Canada, Quebec) in the proximal colon via the catheter or per rectum (Table S1) were observed for 30 minutes; the bisacodyl suspension was made in saline by crushing 2  $\times$  5 mg tablets, with a pestle and mortar for 5 minutes.

### 2.4 | Water perfusion

The water perfusion rate was 0.1 mL/min via each sensor, resulting in a maximum total of 0.5 L/h if all pressure sensors were inside the colon; the pressure was calibrated to 1000 mBar. Each manometry

study would last 6-8 hours, resulting in 3-4 L of water being delivered into the colon. The drainage tube diverted  $1.2 \pm 0.7$  L water ( $N = 18$ ). In addition, water was expelled by the subject through colonic motor activities, in particular HAPWs and SPWs, and water absorption will have taken place. Whether inflow of water for the duration of the 6-8-hour manometry session was affecting intraluminal pressure, that may induce motor patterns, was assessed through the ImageJ-automated comparison of intraluminal pressures made during the baseline period and just before bisacodyl administration as outlined in "statistical analysis" below. Across 19 volunteers, the mean difference in pressure between a period in baseline and a period just prior to bisacodyl administration was  $1.2 \pm 2.0$  mm Hg ( $P = .056$ ), hence no statistically or physiologically significant difference. The subjects were informed about water "leakage" due to propulsive motor patterns, and absorptive pads were provided to give maximal comfort. The discomfort level due to water leakage was different for each subject; from no discomfort at all to some embarrassment with some leakage episodes associated with motor patterns. Comparable results of solid-state and water-perfused catheters have been reported for the detection of HAPWs<sup>26</sup> and cyclic motor patterns.<sup>27</sup>

### 2.5 | Visual identification analysis of motor patterns

Data were not filtered prior to analysis. All data were acquired using the software developed by Medical Measurement Systems (MMS®; Laborie) and analyzed using programs developed by Sean Parsons using ImageJ® (National Institutes of Health, Bethesda) and Matlab® (Mathworks Natick). With an acquisition rate of 10/s in high-resolution manometry, the data were used to calculate the amplitude (mm Hg), interval between successive pressure waves in a cyclic motor pattern occurrence (seconds), propagation velocity (cm/s) and direction (antegrade, retrograde, simultaneous), number of pressure waves within a cyclic motor pattern occurrence, duration (seconds, minutes), and length (cm) in ImageJ. The direction was assessed according to the upstroke of the pressure event. The intraluminal pressures reported (e.g., in the case of cyclic motor pattern amplitude assessment) were relative to the atmospheric pressure outside the colon. ImageJ was also used to conduct FFT analysis to confirm the manual frequency assessment. FFT spectra, with decibel scaling, were calculated for each pressure channel over the time period indicated in the figure legends. Thus pressure (channel, time) maps were converted into spectral-power (channel, frequency) maps. Lastly, Matlab was used to generate the 2D, 3D, and line plot images.

### 2.6 | Motor patterns in the human colon

1. HAPWs: High-amplitude propagating pressure waves. HAPWs are defined as transient increases in pressure of  $>50$  mm Hg (average of all measured pixels within the area of the HAPW) that propagate, almost always in anal direction.<sup>28</sup> They are also referred to in the literature as high-amplitude propagating

contractions or sequences. HAPWs can occur rhythmically at ~1 cpm but it is not a defining characteristic.

2. SPWs: Simultaneous pressure waves. SPWs occur in isolation or following an HAPW; they can occur in a rhythmic fashion at ~2 cpm, but it is not a defining characteristic.<sup>6,7,28,29</sup>
3. CMPs: Cyclic motor patterns. The cyclic motor pattern is defined as a cluster of pressure waves; the pressure waves occur with persistent rhythmicity and propagate over a distance of at least 5 cm. The present study developed a comprehensive analysis of cyclic motor patterns with pressure wave frequencies ranging from 0.3 to 20 cpm. This includes the periodic rectal motor activity at ~3 cpm as described by Rao et al<sup>5</sup> and the cyclic motor pattern extensively reported on by Dinning and co-workers, defined as "repetitive propagating events with a frequency range between 2 and 6 cycles/min"<sup>8,9,30</sup>; we refer to this motor pattern as the "low-frequency cyclic motor pattern." New in the present study is the discovery of a cyclic motor pattern that centers around 11-13 cpm, ranging from 7 to 20 cpm, we refer to this motor pattern as the "high-frequency cyclic motor pattern."
4. Synchronized haustral pressure waves. These occur in a very defined space of 3-5 cm bordered by haustral boundaries.<sup>28</sup> These activities were not taken into account in the present study; their relationship with cyclic motor patterns deserves future studies.

## 2.7 | Statistical analysis

The present study was designed to record the baseline colonic motor activity, which was followed by sessions with different stimuli. It is a descriptive study to document all rhythmic activity in the colon and rectum of healthy volunteers. The stimuli were given consecutively, therefore, data following a stimulus might have been influenced by the remaining activity of the previous stimulus, except the first stimulation (proximal balloon distention (PBD)). Frequency, number of pressure waves, amplitude, propagation velocity and direction, length, and duration were determined for each motor pattern and recording period; the data are given as mean  $\pm$  SD. N represents the number of subjects and n indicates the number of motor patterns. Each parameter noted above was compared as a function of recording period (baseline, proximal balloon distention, meal, and bisacodyl administration) and/or as a function of frequency group (high- vs low-frequency). Duration and number of pressure waves were analyzed and reported per subject or reported overall across all volunteers (the latter mode applied in the reporting of average frequency, amplitude, and length (cm) of cyclic motor patterns). Propagation direction of cyclic motor patterns was compared based on overall presence in each recording period or as a function of colonic location in which the motor pattern was present. Significance of the above parameters was determined by one-way ANOVA with the Bonferroni's correction procedure using Prism 8 software (GraphPad). The Kruskal-Wallis

test was conducted for small sample datasets pertaining to the calculation of cyclic motor pattern duration per volunteer with a follow-up of Dunn's multiple comparison test. Wilcoxon signed-rank test was conducted to assess whether there was a difference in the number of pressure waves before and after a meal per volunteer as a function of high- and low-frequency cyclic motor patterns. Pearson's correlation coefficient test was conducted to assess a potential relationship between the amplitudes of the HAPWs and the amplitudes of the pressure waves in the associated cyclic motor pattern.  $P < .05$  was considered significant.

Potential changes in the intraluminal pressure during the manometry sessions were assessed. In the unfiltered manometry recording, 5-minutes segments were obtained where artifacts impacting colonic pressure were absent (eg, coughing, changing position, bed raised, periods of urination) during baseline and just prior to bisacodyl administration. A segment immediately prior to bisacodyl administration was used given the number of motor patterns present in response to bisacodyl. These segments were analyzed using ImageJ where baseline corrections were made as outlined previously,<sup>31</sup> a Gaussian filter was used with width of the Gaussian defined as 60 seconds. Upon determining the average pressure  $\pm$  SD of the 5-minutes intervals during baseline and immediately prior to bisacodyl administration in each volunteer, a non-parametric Wilcoxon signed-rank test was conducted, given the limited sample size, to assess whether there was a difference in basal intraluminal pressures.  $P < .05$  was considered significant.

The analysis of overall cyclic motor pattern frequency and interval data was carried out with Python in a Jupyter Notebook. Scikit-learn was used for Gaussian kernel density estimation (sklearn.neighbors.KernelDensity) and Gaussian mixture estimation (sklearn.mixture.GaussianMixture). Gaussian kernel density estimation fits the data with a large number (as many as are required to reach fitting tolerance) of Gaussian functions of the same, fixed scale (standard deviation): we used a scale of 1 cpm. Gaussian mixture estimation fits the data with a fixed number of Gaussians (we used 2) with differing scale.

## 2.8 | Determining the position of the sensors

The position of a balloon in all figures is identified by a white line which represents a gap of 10 cm where no data were recorded. The length and velocity of the pressure waves indicated in the figures is accurately reported, taking the balloon position into account. The tip of the catheter was clipped near the ileocecal valve in 15 of 19 volunteers (Table S1). Recording of the anal sphincter pressures made it easy to identify rectal motor activity. The figures mark the location of the first sensor, the position of the balloon(s) and the anal sphincter which were verified by the X-rays taken. A small amount of air was injected into the balloon(s) to facilitate recognition by X-ray. Radiopaque markers were present at channel 1 and at both sides of the balloon(s).



## 2.9 | Impedance cardiography

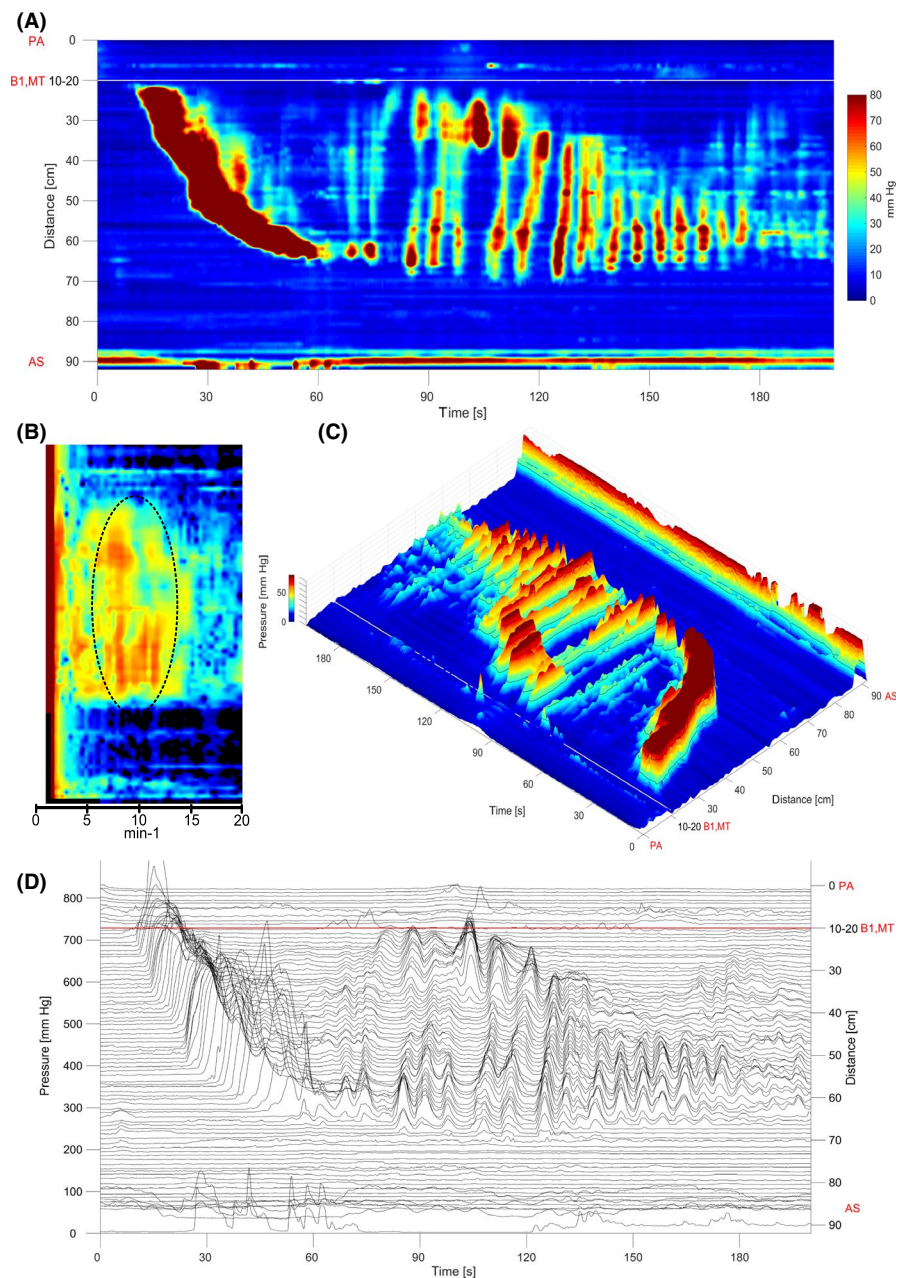
In all subjects, the electrocardiogram and cardiac impedance was recorded to analyze heart rate variability and impedance. In the present study, the only data used from this analysis were the breathing frequency that can be extracted from the impedance measurements. Impedance was recorded by affixing four electrodes in a standard tetrapolar electrode configuration for impedance recording, where two electrodes supplied the constant current source and two electrodes sensed the changes in the transfer impedance. The electrocardiogram was obtained by a standard electrode configuration. Signals were recorded using a MindWare impedance cardio GSC monitor and heart rate variability (HRV) analyzed by MindWare HRV 3.1 and IMP 3.1 software (MindWare Technologies LTD.).

## 3 | RESULTS

### 3.1 | The cyclic motor patterns

Cyclic motor patterns were defined as clusters of cyclic pressure waves with a distinct pressure wave frequency ranging from 0.3 to 20 cpm (Figures 1-4). Incidental clusters of cyclic SPWs or cyclic HAPWs were not classified within the cyclic motor pattern category. Frequency analysis of the cyclic motor patterns showed that there are two groups of cyclic motor patterns, a “low-frequency” and a “high-frequency” pattern (Figure 5; Table 1). This was calculated by measuring the average frequency of the pressure waves within each manually identified cyclic motor pattern (Figure 5A), and by interval analysis of all pressure waves within all cyclic motor patterns (Figure 5B). Both methods showed the same probability of

**FIGURE 1** The high-frequency cyclic motor pattern occurring post-HAPW. (A), (C), and (D). A cyclic motor pattern that follows an HAPW seen in the 2-D, 3-D, and line plot respectively during proximal balloon distention (PBD) with the most proximal sensor (0 cm) in the proximal ascending colon (PA), balloon 1 (B1) in the mid-transverse colon (MT) and anal sphincter (AS) approximately 90 cm from the first sensor. White line and red line in D represent position of the 10 cm balloon. The HAPW average amplitude is 174.0 mm Hg which was cut off in the plots to allow for the visualization of lower-amplitude events. (B) FFT spectrum with a broad peak from 6 to 13 cpm circled with a dotted line. X-axis represents the frequency from 0 to 20 cpm. Y-axis represents the sensors where the vertical scale bar in the spectrum equates to 20 sensors. The FFT analysis was run on the same 140 s duration of the cyclic motor pattern in (A), (C), and (D) following the HAPW. The pressure waves express simultaneous, antegrade, and strong retrograde propagation. This is in contrast to the breathing frequency, which is also commonly expressed at 11-13 cpm but shows exclusively simultaneous events. Breathing frequency noted in this subject was 15 cpm



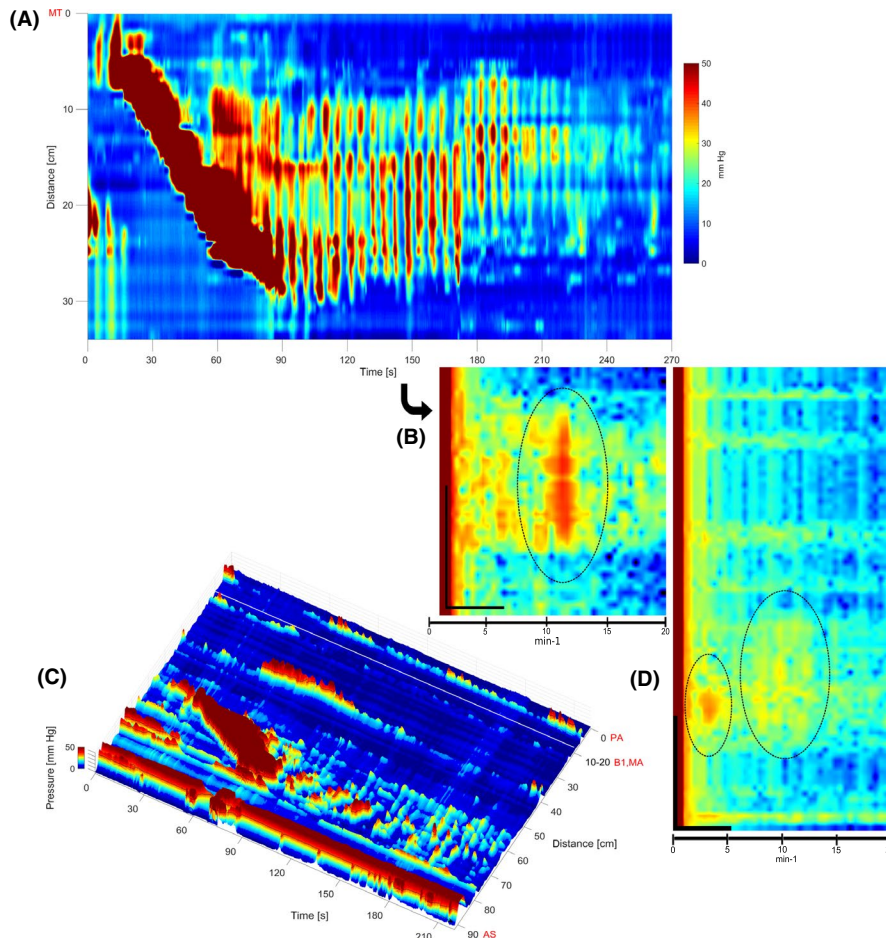


**FIGURE 2** The high-frequency cyclic motor pattern occurring post-HAPW. (A) 2-D plot of a cyclic motor pattern following HAPW during proximal balloon distention (PBD) with the first sensor in the mid-transverse (MT) colon and no balloons. (B) FFT spectrum of (A) with a peak between 11 and 12 cpm circled with a dotted line. X-axis represents the frequency from 0 to 20 cpm. Y-axis represents the sensors where the vertical scale bar in the spectrum equates to 20 sensors. The FFT analysis was run on the same 180 s duration of the cyclic motor pattern in (A) following the HAPW. The HAPW average amplitude was 160.2 mm Hg which was cut off in the plots to allow for the visualization of lower-amplitude events. (C) 3-D plot of a cyclic motor pattern following an HAPW in the distal sigmoid colon during baseline, showing interaction of two distinct frequencies estimated at approximately 3 and 12 cpm. The first sensor is in the proximal ascending colon (PA), with balloon (B1-white line) in the mid-ascending (MA) colon and the anal sphincter (AS) located approximately 95 cm from the first sensor. (D) FFT spectrum of (C) with 2 peaks circled with dotted lines at frequencies of 3.2 cpm and another broad peak from 8-13 cpm. X-axis represents the frequency from 0 to 20 cpm. Y-axis represents the sensors where the vertical scale bar in the spectrum equates to 20 sensors. The FFT analysis was run on the same 130 s duration of the cyclic motor pattern in (C) following the HAPW. The HAPW average amplitude was 174.7 mm Hg which was cut off in the plots to allow for the visualization of lower-amplitude events

a motor pattern belonging to the high-frequency or low-frequency group (Figure 5C). Using the average frequency analysis, the average frequency of the low- and high-frequency cyclic motor patterns was 3.8 and 12.2 cpm, respectively. The interval analysis showed an average frequency of 3.4 and 11.2 cpm, respectively.

Taking the low-frequency pattern as a frequency range of 2-6 cpm<sup>8,13</sup> and the high-frequency range as 7 cpm or higher, the average amplitude of the high-frequency pressure waves,  $22.2 \pm 8.7$  mm Hg, is significantly higher compared to the low-frequency pressure waves at  $16.5 \pm 6.4$  mm Hg (Figure 6F;  $P < .0001$ ). Overall, their direction of propagation, retrograde or antegrade, was not significantly different, with simultaneous propagation dominating (Figure 6A).

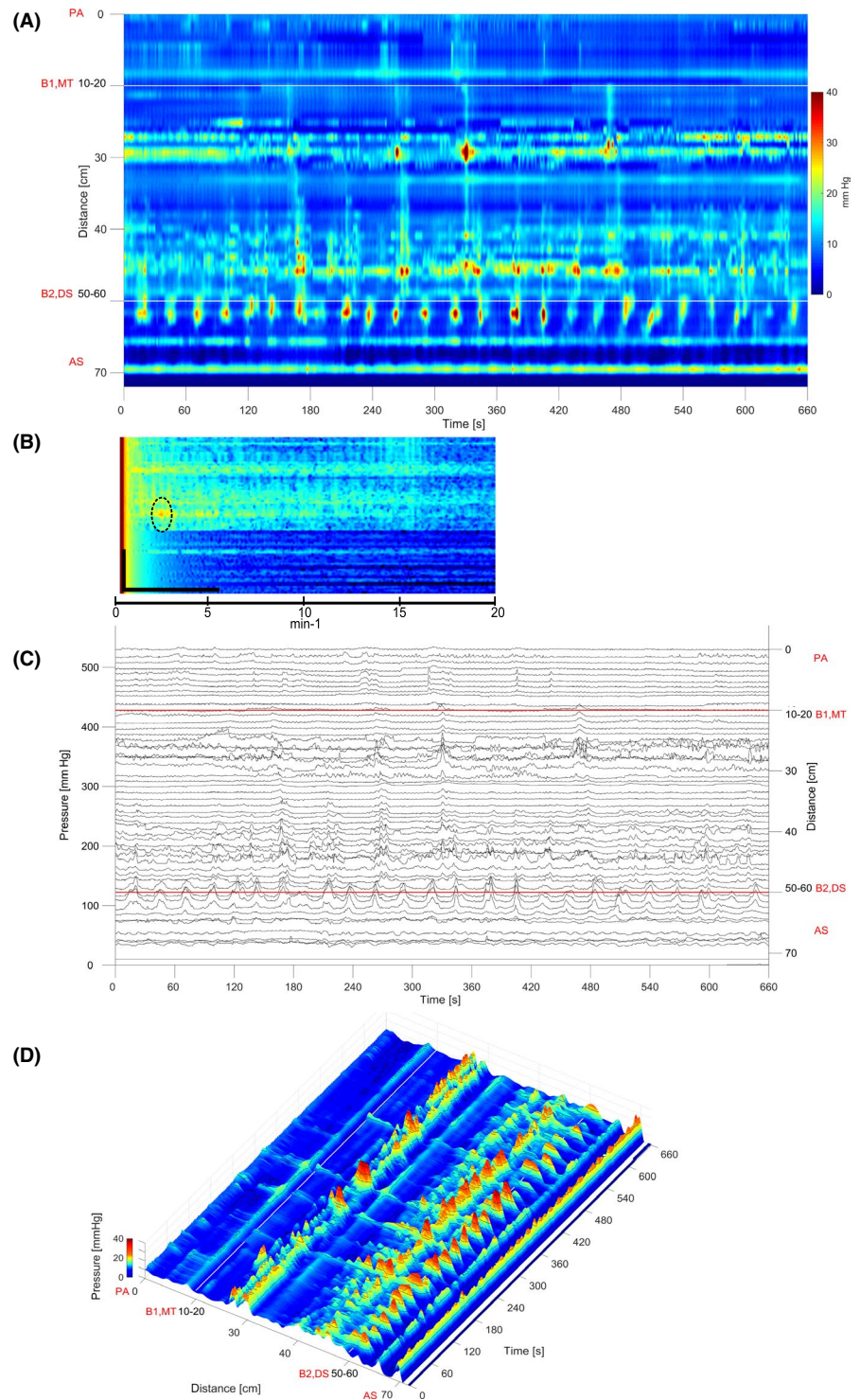
The total number of pressure waves within the cyclic motor patterns per subject was not significantly different before and after the

meal. The total number of pressure wave corresponding to low-frequency cyclic motor patterns in the 90 minutes before the meal was  $33.2 \pm 33.8$  and  $20.5 \pm 18.1$  in the 90 minutes after the meal ( $P = .34$ ). Focusing only on low-frequency retrograde pressure waves, we observed  $19.5 \pm 30.4$  pressure waves per 2 hours per subject during baseline and  $7.2 \pm 14.9$  retrograde pressure waves per 2 hours per subject after a meal ( $P = .86$ ). The total number of pressure wave corresponding to high-frequency cyclic motor patterns in the 90 minutes before was  $30.7 \pm 45.4$  and  $29.0 \pm 44.4$  in the 90 minutes after the meal ( $P = .78$ ).

Three areas were identified where the occurrence of the cyclic motor pattern was prominent (Table 2). (a) A cyclic motor pattern often followed an HAPW (HAPW-CMP) which was dominated by high-frequency pressure waves with frequencies in the range of



**FIGURE 3** The low-frequency (3 cpm) cyclic motor pattern in the rectum. (A) 2-D rectal cyclic motor pattern, primarily retrograde activity at 2.2 cycles/min during baseline with an average length of 4 cm, duration of 660 s. Two white lines represent 10 cm sections of the balloons (B1 and B2). (B) FFT spectrum with a peak at 2.2 cycles per min (cpm) circled with a dotted line. X-axis represents the frequency from 0 to 20 cpm. Y-axis represents the sensors where the vertical scale bar in the spectrum equates to 20 sensors. The FFT analysis was run on the same 660 s duration of the cyclic motor pattern in (A). (C) Line plot of the rectal cyclic motor pattern as seen in (A) operating primarily in the retrograde direction (seen between 60 and 70 cm on the right y-axis). Two red lines represent the balloons (B1 and B2). (D) 3-D plot of (A): rhythmic activity during baseline in the distal sigmoid colon and rectum. Note lack of rhythmic activity preceding the sigmoid colon. Two white lines represent position of 10 cm balloon (B1 and B2). In (A), (C), and (D) the most proximal sensor is located in the proximal ascending colon (PA), balloon 1 (B1) and balloon 2 (B2) are located in the mid-transverse (MT) and distal sigmoid colon (DS), respectively, and the anal sphincter (AS) is located 70 cm from the location of the first sensor



7-20 cpm (Figures 1 and 2). (b) A cyclic motor pattern was prominent in the rectum (rectal-CMP), dominated by low-frequency pressure waves with an average frequency of  $3.3 \pm 2.3$  cpm (range 2-6 cpm). This cyclic motor pattern could be restricted to the rectum but was often congruent with a 3 cpm cyclic motor pattern in the sigmoid (Figure 3). (c) A cyclic motor pattern could occur anywhere throughout the colon (colonic-CMP), but primarily in the transverse, descending, sigmoid colon, not associated with an HAPW; its pressure wave frequency was a mix of low- and

high-frequency cyclic motor patterns, with a range of 0.3-16.3 cpm (Figure 4; Table 2).

### 3.2 | The high-frequency cyclic motor pattern dominates following the HAPW

From the 243 HAPWs observed, 43.6% were followed by a cyclic motor pattern ( $n = 106$ ;  $N = 17$ ; Figures 1 and 2). 82.4% of

the frequencies of the cyclic motor patterns were between 7 and 20 cpm ( $12.8 \pm 3.3$  cpm); 17.6% of the frequencies were between 2 and 6 cpm, as assessed by the percent durations of cyclic motor patterns. The average amplitude of the high-frequency cyclic motor pattern was  $22.7 \pm 8.9$  mm Hg associated with HAPWs of an average amplitude of  $140.0 \pm 50.7$  mm Hg. There was a strong correlation between the amplitude of the HAPW and the amplitude of the pressure waves within the cyclic motor pattern following it ( $P < .0001$ ; Figure 6E). This significance was very evident in the

bisacodyl-induced HAPW and the cyclic motor pattern following it ( $P = .003$ ). The propagation direction of all pressure waves following HAPWs was as follows: 58.9% occurred simultaneously, 24.2% propagated in oral direction and 16.9% in anal direction. There was no statistical difference between the number of oral and anal propagating pressure waves (Figure 6B). Simultaneous propagation was the most common direction in the transverse, descending and sigmoid colon (70.8%, 54.5%, 51.1%, respectively) in any occurrence of the cyclic motor pattern. There was no difference in the percentage

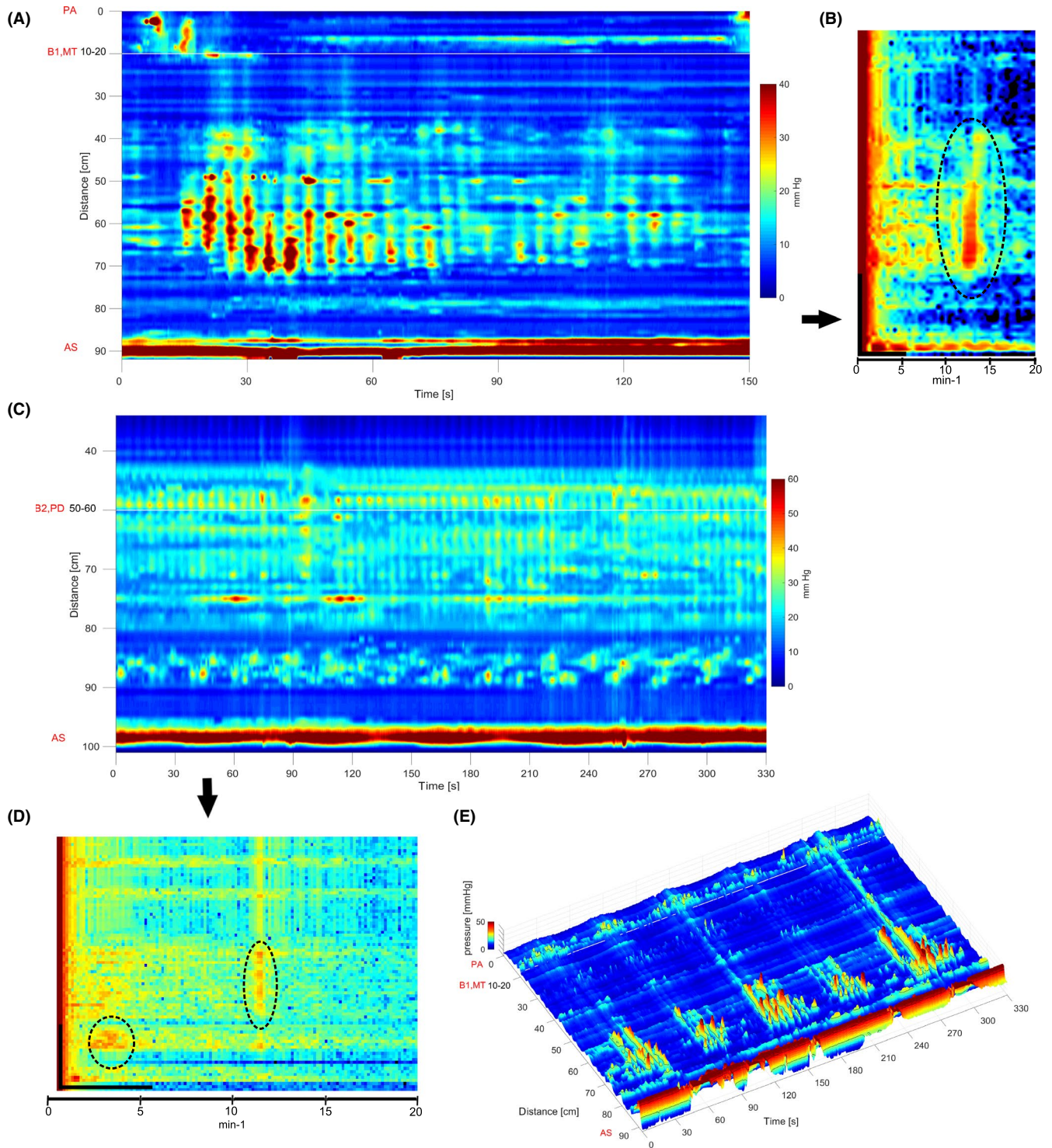




**FIGURE 4** The high-frequency colonic cyclic motor pattern. (A) 2-D plot of colonic cyclic motor pattern in the descending and sigmoid colon during proximal balloon distention (PBD); the first sensor is in the proximal ascending colon (PA), and the balloon (B1) is located in the mid-transverse (MT) colon with the anal sphincter (AS) located approximately 90 cm from the most proximal sensor. White line represents positioning of 10 cm balloon. (B) FFT spectrum of (A) with peak centered at 12.7 cpm corresponding to the colonic cyclic motor pattern. X-axis represents the frequency from 0 to 20 cpm. Y-axis represents the sensors where the vertical scale bar in the spectrum equates to 20 sensors. The FFT analysis was run on the same 130 s duration of the cyclic motor pattern in (A). (C) 2-D plot of a high-frequency colonic-CMP occurring in the distal colon, during baseline, with a concomitant presence of the low-frequency rectal-CMP and 1 cpm anal sphincter oscillations. The first sensor is in the mid-ascending colon; the balloons, B1 and B2, are located in the distal ascending and proximal descending colon (PD), respectively, with the anal sphincter (AS) located approximately 97 cm from the proximal most sensor. This figure does not illustrate the location of the first sensor and the proximal balloon location as they were omitted to allow for the clear visualization of the shown motor patterns. (D) FFT spectrum of (C) with a low-frequency peak centered at 2.7 cpm corresponding to the cyclic motor pattern in the rectum, and a high-frequency peak at 11.1 cpm representative of the high-frequency colonic cyclic motor pattern. X-axis represents the frequency from 0 to 20 cpm. Y-axis represents the sensors where the vertical scale bar in the spectrum equates to 20 sensors. The FFT analysis was run on the same 330 s duration of the cyclic motor pattern in (C). (E) 3-D plot of the rhythmicity of colonic-CMP clusters appearing at 1 cpm, originating in the proximal colon. The proximal most sensor is in the proximal ascending colon (PA); the balloon is present in the mid-transverse colon (MT) and the anal sphincter (AS) is located approximately 85 cm from the first sensor. The pressure waves within a single cluster of the colonic-CMP in the sigmoid colon displayed high-frequency (10–12 cpm). White line represents positioning of 10 cm balloon (B1)

of antegrade and retrograde propagation directions within a location, and no statistical difference in the appearance of a particular direction in any location of the colon.

The average length and duration of the cyclic motor patterns that followed the HAPWs were  $15.8 \pm 8.1$  cm and  $76.2 \pm 53.3$  seconds, respectively (Table 2). When comparing different locations along the colon, the average frequencies did not differ significantly; transverse  $11.9 \pm 3.3$  cpm ( $n = 51$ ), descending  $11.3 \pm 4.3$  cpm ( $n = 19$ ), and sigmoid  $11.1 \pm 5.1$  cpm ( $n = 42$ ).

The individual pressure waves within the cyclic motor pattern were almost always occurring without interruption but occasionally a clear segmentation pattern was observed, that is, the wave consisted of a pressure-relaxation cycle (Figure 2C), resulting in a checkered pattern of isolated pressure transient, identical in appearance to the classic Cannon-type segmentation in the small intestine.<sup>32</sup> This occurred when the low- and high-frequency cyclic motor patterns appeared in the same section of the colon. The pattern was distinctly seen in the distal colon amidst propagating and simultaneous pressure waves.

### 3.3 | Distinguishing the high-frequency cyclic motor pattern from the breathing frequency

In most subjects, breathing was identifiable as background simultaneous pressurizations at the breathing frequency established by manually counting breaths per minute, and through the impedance measurements which were obtained simultaneously with the manometry assessment. In 10 subjects with a cyclic motor pattern pressure wave frequency of  $12.0 \pm 1.2$  cpm, the breathing frequency ranged from 15 to 18 cpm. Figure 7 shows that a subject with a breathing frequency of 15 cpm identified by background and impedance had a concomitant pressure wave frequency of 12 cpm. Another distinct feature of the high-frequency cyclic motor pattern is that it shows direction of propagation, that is, any cyclic motor pattern consists of a mixture of simultaneous, retrograde and antegrade

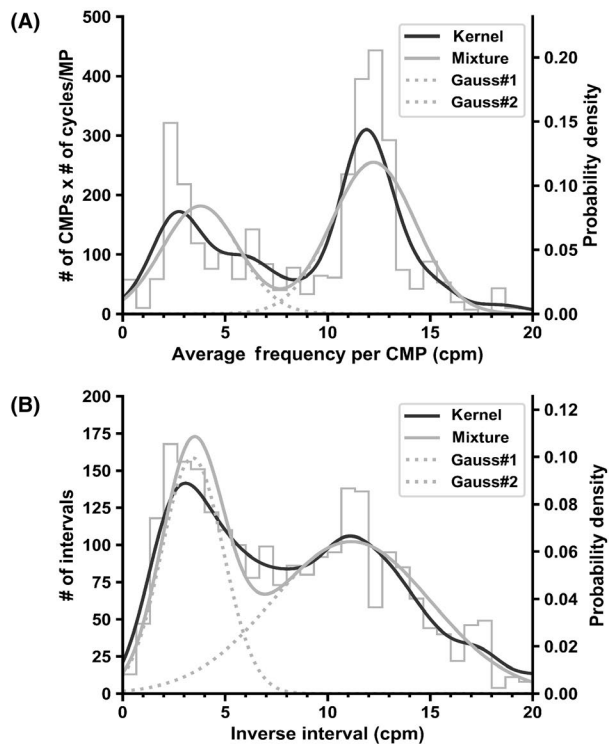
propagating pressure waves, whereas the breathing frequency artifact always showed exclusively simultaneous pressure changes. Figure 1 shows a typical motor pattern with distinct antegrade or retrograde propagation, in stark contrast to the simultaneous pressurizations as the hallmark of the breathing artifact.

### 3.4 | The low-frequency cyclic motor pattern in the rectum

The rectal cyclic motor pattern (Figure 3) was present in 14 subjects, occurring a total of 37 times, most prominent during baseline ( $N = 8$ ,  $n = 15$ ), and meal periods ( $N = 6$ ,  $n = 11$ ), although it was also present during balloon distention ( $N = 5$ ,  $n = 7$ ) and bisacodyl ( $N = 3$ ,  $n = 4$ ). The overall amplitude of the cyclic motor pattern in the rectum was  $18.0 \pm 5.6$  mm Hg (Table 2). The rectal cyclic motor pattern presented a combination of simultaneous, antegrade and retrograde propagation. The most prominent propagation direction was retrograde representing ~50.2% of total propagation overall, followed by simultaneous direction at 32.8% and antegrade at 16.9%. The overall propagation velocities for retrograde and antegrade direction were found to be  $0.82 \pm 0.77$  cm/s and  $1.10 \pm 1.10$  cm/s respectively, not significantly different. Only during baseline was the retrograde direction more prominent compared to the antegrade activity (Figure 6C;  $P < .001$ ). The average length and duration of the rectal cyclic motor pattern were  $5.7 \pm 2.5$  cm and  $6.0 \pm 4.9$  minutes, respectively (Table 2).

### 3.5 | The colonic cyclic motor pattern not associated with HAPWs

The colonic cyclic motor pattern, not associated with HAPWs was observed in 18 subjects ( $n = 107$ ; Figure 4), most prominently found during baseline ( $N = 16$ ,  $n = 47$ ) and meal periods ( $N = 12$ ,  $n = 29$ ). Three quarters of this activity originated in the descending or



Gaussian mixture estimation of all cyclic motor pattern frequency data.

Data	Gaussian components		
	Mean (cpm)	SD (cpm)	Area under curve (probability)
Average frequency per CMP	3.79	1.87	0.39
	12.24	2.04	0.61
Inverse interval	3.41	1.50	0.38
	11.15	3.88	0.62

**FIGURE 5** Analysis of cyclic motor pattern frequency by average frequencies and intervals. (A) All cyclic motor patterns were identified, the average frequency of each individual cyclic motor pattern occurrence calculated and the number of pressure waves corresponding to the average frequency noted. The histogram (stepped gray line) shows the number of CMPs with a particular average frequency, multiplied by (ie, weighted by) the number of pressure waves present in the occurrence (left y-axis). If the histogram is scaled such that its total area is equal to one, the relevant height scale is the probability density (right y-axis) which indicates the probability of a CMP having the particular frequency. The histogram was modeled (fitted) by a sum of Gaussian distributions. In Gaussian kernel density estimation (dark smooth line) the histogram is fitted with as many Gaussians as are required for a good fit, but they all have the same width (standard deviation; here set to 1.0 cpm). In Gaussian mixture estimation (light smooth lines) the histogram is fitted with a fixed number of Gaussians (here 2; dotted lines) of any width. (B) The interval between every pressure wave in every CMP is measured and is converted into a frequency (1/interval). The histogram (stepped gray line) shows the number of intervals with a particular frequency (left y-axis). As in (A) the right y-axis shows the corresponding probability density scale and the data is fitted with a Gaussian kernel density estimate (1.0 cpm SD) and a Gaussian mixture estimate of two components. (C) reports the parameters of the two Gaussians (dotted lines) in (A) and (B)

sigmoid colon whereas 25% originated more proximally. The colonic motor pattern episodes would also occur simultaneously with rhythmic activity in the rectum (Figure 4C). The propagation direction of

the pressure waves across all the colonic cyclic motor patterns was predominantly simultaneous (47%), followed by retrograde (26%) and antegrade (27%) pressure waves. When different interventions and different sites of origin were compared, there were no significant differences between antegrade and retrograde directionality of the pressure waves (Figure 6D; Table 2). The mean propagation velocity was  $6.6 \pm 5.8$  cm/s and  $5.2 \pm 6.7$  cm/s for antegrade and retrograde propagation, respectively, not significant different. The length (along the colon) and duration (of the cyclic motor pattern cluster) were both highly variable at  $20.1 \pm 13.5$  cm and  $5.0 \pm 10.0$  minutes, respectively (Table 2). The colonic cyclic motor pattern itself also occurred in a rhythmic fashion ( $N = 9$ ,  $n = 17$ ) at  $1.4 \pm 0.5$  cpm with a range of 0.5–2.3 cpm (Figure 4E). Most pressure waves associated with colonic cyclic motor patterns that were not associated with HAPWs belonged to the high-frequency category. The proportion of total pressure waves associated with low- and high-frequency cyclic motor patterns were 37.2% and 62.8%, respectively.

### 3.6 | Comparison between the cyclic motor patterns in the rectum, colon, and following the HAPWs

Taking all pressure wave frequencies into account, we compared the cyclic motor pattern characteristics in the rectum, colon, and following HAPWs (Table 2). The pressure waves following the HAPW possessed much higher amplitudes than those within the colonic cyclic motor pattern ( $P = .0002$ ) and within the rectum ( $P = .0088$ ). The largest increase in amplitude across all cyclic motor patterns was from baseline to bisacodyl, specifically in cyclic motor patterns following the HAPW ( $P = .0264$ ) and within the colonic cyclic motor pattern ( $P < .0001$ ), while there were no interventional effects on rectal cyclic motor pattern amplitudes. The cyclic motor patterns in the colon and following the HAPW had the greatest proportion of simultaneous propagation. In addition, both the retrograde and antegrade proportions of the HAPW and colonic cyclic motor patterns were significantly less than the retrograde proportions found in rectal cyclic motor pattern ( $P < .05$  overall). The durations and lengths of the cyclic motor pattern differed (Table 2). The colonic cyclic motor pattern was on average present for the longest duration when compared to the durations of the rectal cyclic motor pattern ( $P = .002$ ) and the cyclic motor patterns following the HAPW ( $P = .0006$ ). The rectal cyclic motor pattern was the shortest motor pattern in terms of length when compared to colonic cyclic motor pattern ( $P < .0001$ ) and the cyclic motor patterns following the HAPW ( $P < .0001$ ).

## 4 | DISCUSSION

The present study shows that in addition to the low-frequency cyclic motor pattern, defined previously as clusters of pressure waves between 2 and 6 cpm,<sup>8,9</sup> the colon exhibits a prominent high-frequency cyclic motor pattern that is often seen in the wake of a high-amplitude propagating pressure wave (HAPW) but is also seen throughout the transverse, descending, and sigmoid colon as an isolated motor pattern. The high-frequency cyclic motor pattern centers

**TABLE 1** Comparison of the cyclic motor patterns of the human colon

	Low-Frequency CMP (2-6 cpm)	High-Frequency CMP (7-20 cpm)
Frequency	3.6 ± 1.7 cpm	12.4 ± 1.8 cpm
Number of pressure waves/ subject		
Mean ± SD	12.2 ± 7.5 pressure waves	14.0 ± 14.1 pressure waves
Min-Max	3-35 pressure waves	3-107 pressure waves
25th-75th percentile	6-15.75 pressure waves	6-17 pressure waves
Pressure wave amplitude		
Mean ± SD	16.5 ± 6.4 mm Hg****	22.2 ± 8.7 mm Hg
Min-Max	2.5-40.7 mm Hg	8.5-75.2 mm Hg
25th-75th percentile	12.4-20.5 mm Hg	16.7-26.0 mm Hg
Pressure wave propagation direction		
Percent direction per CMP episode (mean ± SD)	Simultaneous: 47.4 ± 33.8%	Simultaneous: 59.9 ± 33.4%
	Anterograde: 22.3 ± 29.3%	Anterograde: 19.7 ± 24.1%
	Retrograde: 30.4 ± 32.8%	Retrograde: 20.5 ± 25.3%
CMP duration/subject		
Mean ± SD	296.3 ± 355.3 s	99.8 ± 218.5 s
Min-Max	20 s-47 min	14 s-38 min
25th-75th percentile	90-390 s	33-105 s

Note: The values for the 25th and 75th percentiles were included to report where the majority (50%) of the data was present without the impact of potential outliers that may be present in the min and max values stated in the table above.

Asterisk represents the comparison between cyclic motor patterns belonging to the high- and low-frequency ranges.

\*\*\*\* $P < .0001$ .

around 11-13 cpm. It is rarely reported on in human colonic manometry studies, but noted in early research. Code<sup>33</sup> reported in 1952 type 1 waves in the human colon, described as simple monophasic waves that had the highest rhythmic frequency characteristic for the colon at 13 cpm, in addition to waves at 3-8 cpm. Kerlin, Zinsmeister, and Phillips<sup>34</sup> reported colonic frequencies which they could not distinguish from respiratory artifacts. Due to this uncertainty, in many studies, rhythmic activity that was deemed to be potentially caused by respiration in the frequency range of 8-12 cpm, was not analyzed.<sup>35-37</sup> In other studies, frequencies between 16 and 20 cpm were deemed potential respiratory movements and removed from the analysis.<sup>4,13,30,38</sup> Other studies defined the cyclic motor pattern by its frequency range from 2 to 6 cpm and hence did not analyze data > 6 cpm.<sup>30</sup> We did not filter our data nor did we exclude any frequency domain. We did carefully identify artifacts due to body movements and removed those from the analysis. We show that pressure waves within the high-frequency cyclic motor patterns are not caused by breathing since the pressure waves caused by breathing, which were always visible in the background, had a distinctly different frequency as determined by impedance measurements and manual assessments, and was usually 15-16 cpm. Furthermore, the individual pressure waves within the high-frequency cyclic motor

patterns always showed a percentage of antegrade or retrograde propagation, which was never seen in breathing artifacts.

The occurrence of the high-frequency cyclic motor pattern with rhythmicity between 9 and 15 cpm is consistent with human colon electrophysiological studies that showed a prominent presence of slow waves within this frequency range. Sarna et al recorded with serosal electrodes during surgery and found a frequency of 11.4 cpm to be extensively present (see figure 2 in ref. 14). Bueno et al found a prominent presence of cyclic electrical activity between 10 and 12 cpm.<sup>15</sup> Couturier et al found the most prominent frequency between 8.4 and 10.6 cpm,<sup>39</sup> similar to Schang and Devroede, their average was 10 cpm.<sup>40</sup> Consistently, in vitro studies of the human colon circular muscle showed prominently a slow wave activity in a similar frequency range.<sup>16,41,42</sup> Hence, the pressure wave pattern will be caused by rhythmic circular muscle contractions generated by short bursts of smooth muscle action potentials superimposed on slow wave activity in the 9-15 cpm range. The slow waves are generated by one of the dense networks of interstitial cells of Cajal.<sup>16,43,44</sup> Human and animal studies have shown that, in contrast to the stomach and small intestine, the colon pacemaker activity is labile and does not show a persistent frequency gradient.<sup>45</sup> If the frequency is "noisy," that is, if it fluctuates around, for example, 12 cpm, both at



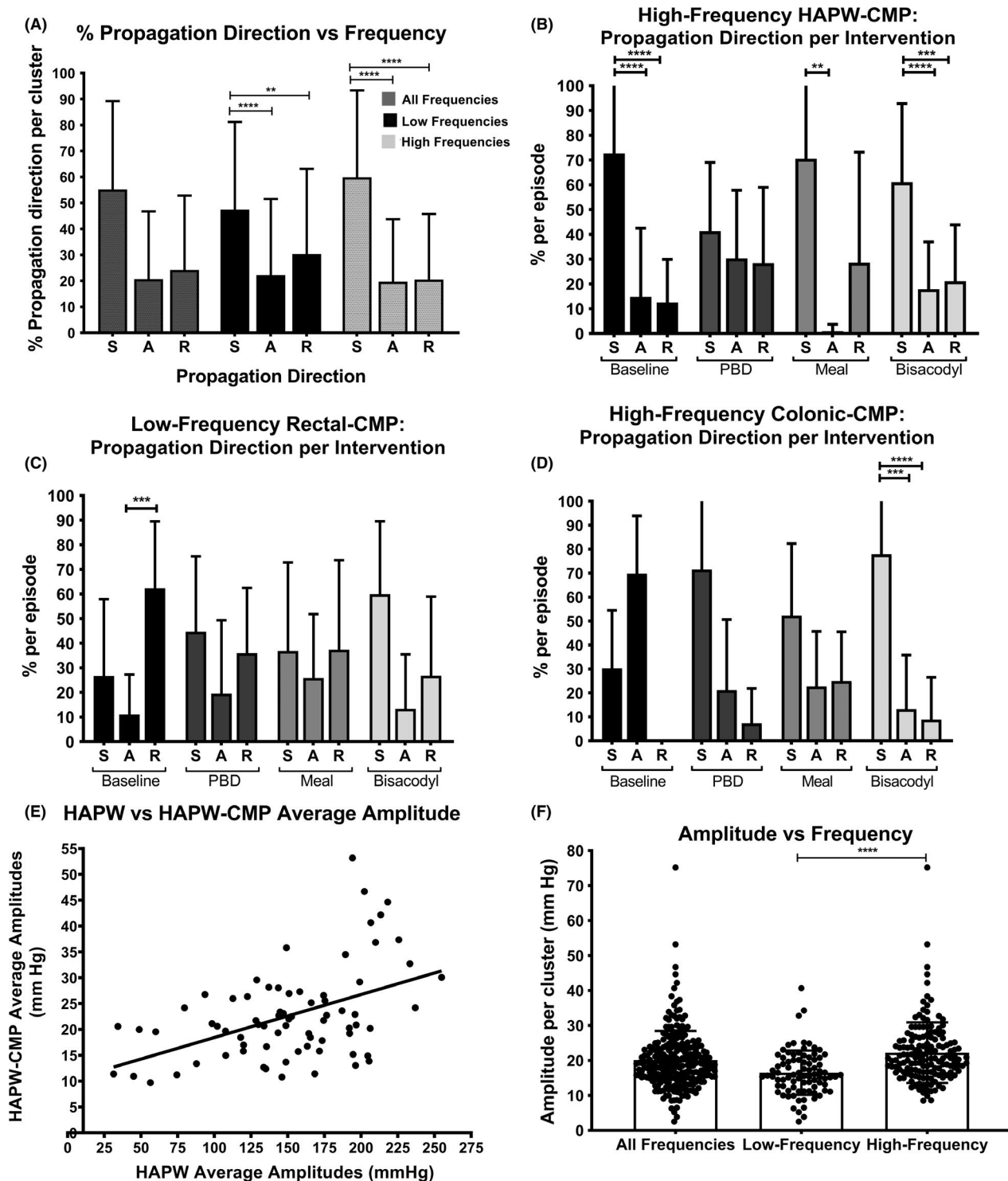


**FIGURE 6** Features of the cyclic motor patterns. (A) Propagation direction (simultaneous (S), antegrade (A) and retrograde (R)) reported as a function of high- and low-frequency groups, and as a combination of all frequencies. Note within each frequency group, simultaneous propagation is most prominent while no statistically significant difference exists between the two frequency groups nor between antegrade and retrograde propagation within the frequency groups. (B) Propagation direction reported as percent of pressure waves per cluster of high-frequency cyclic motor patterns following HAPWs. (C) Propagation direction reported as percent of pressure waves per cluster of rectal-CMP. (D) Propagation direction reported as percent of pressure waves per cluster of high-frequency colonic cyclic motor patterns. (E) Amplitude correlation of all HAPWs and their corresponding cyclic motor patterns (Pearson's correlation coefficient = 0.4662;  $P < .0001$ ). (F) Average amplitude of pressure waves per cluster of all CMPs and those categorized as the high- and low-frequency cyclic motor patterns. The y-axis reports the average pressure (mm Hg) of the pressure waves within the clusters. Each point represents a cluster of the CMP's. \*\*\*\* $P < .0001$ , \*\*\* $P < .001$ , \*\* $P < .01$ , \* $P < .05$

**TABLE 2** Comparison of the cyclic motor patterns in the colon and rectum without separation in high- and low-frequency categories

	HAPW-CMP	Colonic-CMP	Rectal-CMP
Pressure wave frequency			
Mean $\pm$ SD	11.6 $\pm$ 4.2 cpm****	8.1 $\pm$ 4.4 cpm <sup>a/####</sup>	3.3 $\pm$ 2.3 cpm****
Min-Max	3.3-20 cpm	0.3-16.3 cpm	0.6-12 cpm
25th-75th percentile	9.1-13.7 cpm	3.9-12.0 cpm	2.3-3.3 cpm
Pressure wave amplitude			
Mean $\pm$ SD	22.7 $\pm$ 8.9 mm Hg***	18.2 $\pm$ 6.4 mm Hg	18.0 $\pm$ 5.6 mm Hg**
Min-Max	9.7-78.2 mm Hg	3.4-38.3 mm Hg	2.5-32.8 mm Hg
25th-75th percentile	18.8-26.4 mm Hg	14.5-21.7 mm Hg	15.0-21.7 mm Hg
Percent direction per CMP episode (mean $\pm$ SD)			
Pressure wave propagation direction	Simultaneous: 47.1 $\pm$ 31.7%	Simultaneous: 58.6 $\pm$ 33.3%	Simultaneous: 36.7 $\pm$ 32.8%
	Anterograde: 26.7 $\pm$ 29.3%	Anterograde: 16.5 $\pm$ 22.3%	Anterograde: 17.2 $\pm$ 22.8%
	Retrograde: 26.2 $\pm$ 29.8%	Retrograde: 24.9 $\pm$ 28.3%	Retrograde: 46.1 $\pm$ 32.4%
Pressure wave length			
Mean $\pm$ SD	15.8 $\pm$ 8.1 cm*	20.1 $\pm$ 13.5 cm####	5.7 $\pm$ 2.5 cm****
Min-Max	4-45 cm	3-68 cm	3-13 cm
25th-75th percentile	10-21 cm	8-27 cm	4-7 cm
CMP duration			
Mean $\pm$ SD	1.3 $\pm$ 0.9 min****	5.0 $\pm$ 10.0 min	6.0 $\pm$ 5.0 min**
Min-Max	14 s-4.3 min	15 s-74 min	40 s-24 min
25th-75th percentile	35-105 s	47 s-5.5 min	2.5-8.0 min

Note: All \* represent comparisons between HAPW- and Colonic-CMP; All # represent comparisons between Colonic- and Rectal-CMP. All ♦ represent comparisons between HAPW- and Rectal-CMP. Four symbols =  $P < .0001$ . Three symbols =  $P < .001$ . Two symbols =  $P < .01$ . One symbol =  $P < .05$ . The values for the 25th and 75th percentiles were included to report where majority (50%) of the data was present without the impact of potential outliers that may be present in the min and max values stated in the table above.

<sup>a</sup>This value reflects a combination of low-frequency and high-frequency activity.

the proximal and distal end of the cyclic motor pattern activity, propagation direction will be “chaotic” and can switch direction quickly and can occur simultaneous; in a system of coupled oscillators, the propagation is not determined by sequential depolarization of consecutive cells but rather by the synchronization of cyclic electrical activities with or without phase lags.<sup>46-49</sup> The high-frequency cyclic motor pattern consists of rather randomly alternating retrograde and antegrade propagating, or simultaneous pressure waves. The electrical activity underlying simultaneous pressure waves can be synchronized slow wave activity without phase lag, or slow wave activity at a very high apparent velocity. In the rabbit colon, where we recorded contractile activity and pressure waves simultaneously, simultaneous pressure waves were often associated with clusters of contractions that propagated at high velocity.<sup>50</sup> Mixed direction of propagation is likely associated with net non-propulsive activity promoting absorption and storage.<sup>51,52</sup>

The present study uses a water-perfused catheter over a period of 6-8 hours. A consideration is whether or not the water perfusion would lead to colonic distention that might introduce motor activity. We observed no significant increase in baseline pressure over the duration of the study. Furthermore, the high-frequency cyclic motor pattern was often seen during baseline with features no different from patterns observed later in the recording. The colon has a large

capacity to absorb water and water was expelled by the many propulsive motor patterns and some water was drained out via a rectal catheter. Importantly, a frequency spectrum of cyclic activity in the human colon obtained using a fiber optics catheter also showed peaks at ~3 and ~11 cpm, see figure 2 in ref. 53. In general, comparison between studies that use water-perfused or solid-state catheters shows no significant differences.<sup>27</sup>

Many human manometry studies have shown an increase in motility in response to a meal, in particular an increase in HAPWs.<sup>5,11,13,34,37,54-57</sup> Dinning et al reported that retrograde propagating cyclic motor patterns at 2-6 cpm occurred on average 5.6 times per 2 hours during baseline, which changed after a meal to 34.7  $\pm$  19.8 per 2 hours.<sup>8,13,38</sup> This impressive post-prandial increase in the low-frequency cyclic motor pattern became a benchmark for normal colonic response parameters,<sup>58</sup> which was then implemented in a later study<sup>4</sup> assessing colonic motor abnormalities in slow transit constipation. It was concluded that in patients with STC, on average, the occurrence of the low-frequency cyclic motor pattern did not show a difference before and after a meal although in 5 out of 14 patients, the meal initiated the cyclic motor pattern when no pattern was present during baseline (table 1 in ref. 4); hence the absence of a meal response does not appear to be a consistent feature in patients with constipation. Relatedly, Bassotti et al<sup>59</sup> reported an

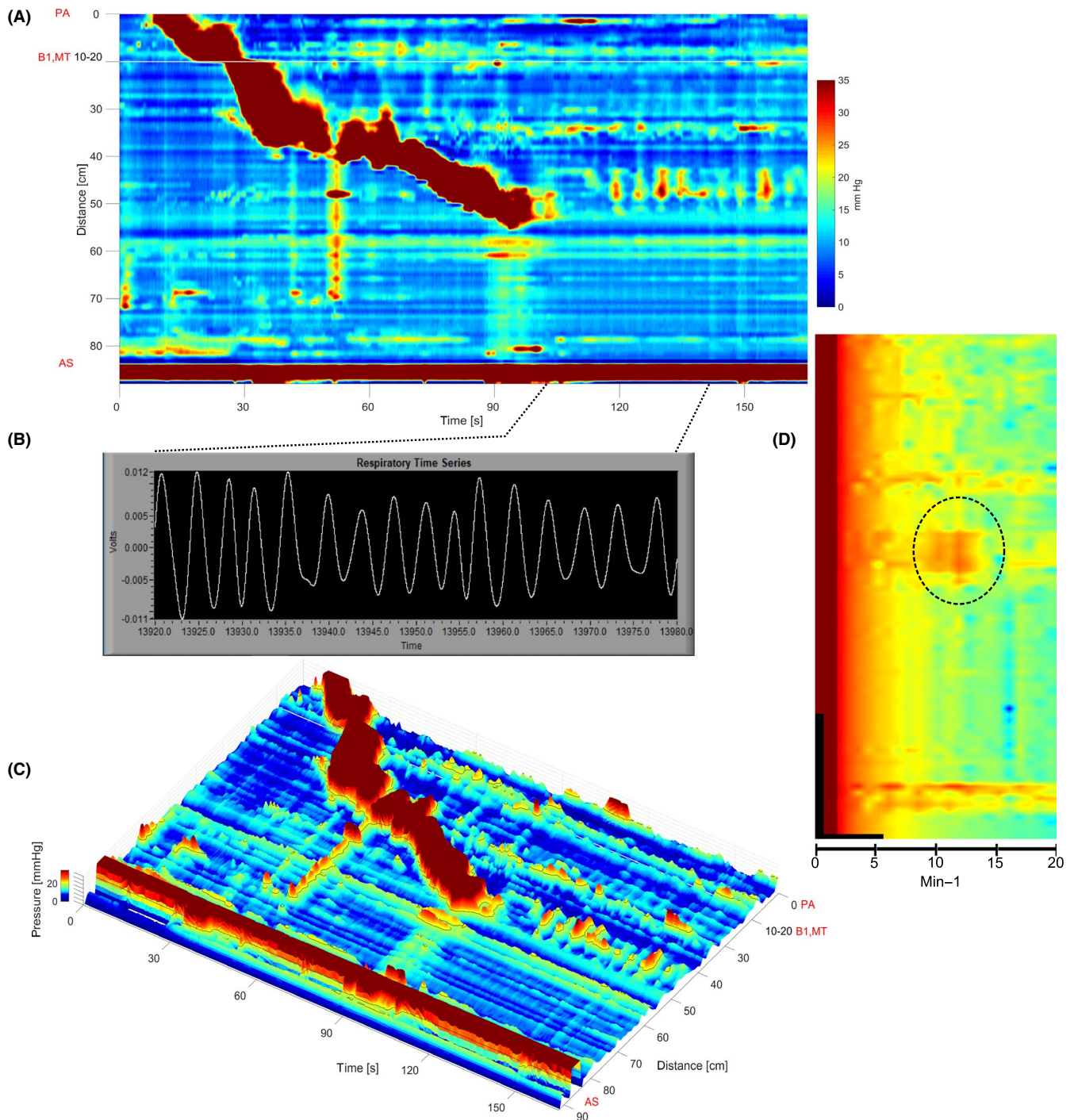


**FIGURE 7** The high-frequency cyclic motor pattern is distinct from breathing artifacts. (A) 2-D plot: HAPW-CMP during the meal intervention with the most proximal sensor in the proximal ascending colon (PA), a balloon (B1) at the mid-transverse colon (MT) and the anal sphincter (AS) approximately 85 cm from the proximal sensor. The white line represents positioning of 10 cm balloon. (B) Respiratory Time Series: y-axis reports the change in voltage with a maximal change of 23 mV; x-axis reports the time of the recording in seconds which is used to time match with the segment of the cyclic motor pattern in the HRCM recording in (A) seen by the two dotted lines. The impedance recording directly corresponds to the low-amplitude background frequency seen between 60 and 80 cm (left y-axis in (A)), thereby providing evidence that the breathing is 16 cpm. (C) 3-D plot of HAPW-CMP in (A). The true HAPW average amplitude was 110.0 mm Hg which was cut off in the plot to allow for the visualization of lower-amplitude events. (D) FFT spectrum of (A) and (C) with peak centered at 11.8 cpm corresponding to the cyclic motor pattern following HAPW. X-axis represents the frequency from 0 to 20 cpm. Y-axis represents the sensors where the vertical scale bar in the spectrum equates to 20 sensors. The FFT analysis was run on the same 60 s duration of the cyclic motor pattern in (A) and (C) following the HAPW



increase in regular rhythmic activity with a dominant frequency of 3 cpm from 10% to 34% in patients with slow transit constipation after a meal compared to the period preceding the meal. The present study shows that although some subjects showed an increase in the low-frequency cyclic motor pattern and some showed an increase in the high-frequency cyclic motor pattern, on average there was no significant difference before and after meal intake. This means that the absence of a meal response in a patient with constipation should probably not be seen as an abnormal feature and does not necessarily indicate pathophysiology.

In the present study, the rectal cyclic motor pattern was predominantly retrograde and around 3 cpm. Rao et al,<sup>12</sup> comparing activity at 7 cm (rectum) to 14 cm (sigmoid) from the anus, found that the clusters of rectal cyclic motor activity to be 14% retrograde and 47% simultaneous, whereas at night time it was 16% simultaneous and 36% retrograde. This analysis is different from the present study and other studies using high-resolution manometry where the characteristics of the individual pressure waves can be analyzed which is not possible with low resolution manometry. In the present study, the presence of the rectal cyclic motor pattern was quite variable (it occurred in 66% of 21 healthy volunteers) and did not, on average, increase with a meal.<sup>12</sup> It was proposed to be an intrinsic braking mechanism preventing untimely flow of colonic contents into the rectum, particularly during sleep.<sup>12</sup> Patients with slow transit constipation showed a 50% increase in this rectal cyclic motor pattern and the hypothesis was put forward that an increase in the rectal cyclic motor activity may contribute to the pathogenesis of slow transit constipation.<sup>9</sup> The rectosigmoid brake hypothesis was supported by studies from Lin et al<sup>8</sup> pointing to the prominence of retrograde propagation in the sigmoid and rectum. This motor pattern was very strong and persistent in the distal colon in patients after surgery involving right hemicolectomy<sup>30</sup> suggesting that it may serve to restore normal bowel function.<sup>8</sup> Interestingly, the pattern shows all the characteristics of a network of pacemaker cells, coupled oscillators, underlying it (see figure 3 in ref. 30), such as a frequency gradient, patterns of Cannon-type segmentation and dislocations (the sudden disappearance of a pressure wave), as reported on recently, based on comparisons between recorded slow wave activity and a mathematical model of coupled oscillators.<sup>49,60</sup>

Giorgio et al<sup>3</sup> came to the conclusion that simultaneous presurizations found between bisacodyl-induced HAPWs were a biomarker of neuromuscular pathology in children with constipation since it was not observed in children who were deemed not to have constipation based on HRCM features and subsequent assessments. In the present study in adults from 19 years of age and older, 4.5% of the HAPWs during all interventions across all healthy volunteers were followed by absolute quiescence (and 5.4% post-bisacodyl), whereas 43.6% of HAPWs were followed by a cyclic motor pattern (and 36.6% post-bisacodyl). Because of the prominence of post-HAPW cyclic motor patterns in healthy subjects, it appears that this cyclic motor pattern is not a unique feature of constipation in adults. The cyclic motor pattern that follows the HAPWs is primarily

high-frequency, which may explain why Lin et al did not find a correlation between HAPWs and cyclic motor patterns as they analyzed only the 3 cpm cyclic motor pattern.<sup>8</sup>

The high-frequency oscillator and low-frequency oscillator are likely coming from two different ICC networks, since we saw these cyclic motor patterns operate in the same spatial and temporal region in the distal sigmoid colon overlapping with one another (Figure 2C). Interestingly, where these two distinct frequencies overlap, there is sometimes evidence of the Cannon-type segmentation pattern similar to the small intestine where we showed that this segmentation pattern is caused by phase-amplitude coupling of two oscillators.<sup>32</sup>

In summary, the human colon has two prominent cyclic motor patterns, clusters of pressure waves centering on 3-4 and 11-13 cpm. Within almost all clusters, pressure waves show a mix of antegrade, retrograde, and simultaneous propagation, likely to move content in alternating directions. We proved the high-frequency pattern to be unrelated to breathing. This pattern should be regarded as a prominent feature of normal colon motility likely associated with segmentation (absorption and storage) and maintenance of continence.

## ACKNOWLEDGMENTS

JDH received a Canadian Foundation for Innovation John Evans Leadership grant for the equipment used in this study. Operating funds were obtained from the Hamilton Academic Health Sciences Organization (HAHSO) to ER and from the Canadian Institutes of Health Research (CIHR) to JDH. The Farncombe Family Digestive Health Research Institute provided partial salary support for J-HC and SPP. The hardware was designed in collaboration with Medical Measurement Systems, in particular Jan Willem van der Wal. The catheters were designed in collaboration with Howard Mui and staff at Mui Scientific.

## DISCLOSURE

No competing interests declared.

## AUTHOR CONTRIBUTIONS

HRCM was developed by J-HC and JDH. All HRCM studies were executed by J-HC. All analysis for the present study was executed by MP. MP made significant contributions to data acquisition and data interpretation and wrote the first extensive draft of the paper. SPP made significant contributions to data acquisition, data analysis, and interpretation. ER obtained funding and was involved in aspects of data interpretation. The identification and characterization of the motor patterns described here was the result of extensive discussions between all authors. All authors discussed and revised the manuscript and approved the final version.

## ORCID

Maham Pervaz  <https://orcid.org/0000-0002-9004-2778>

Ji-Hong Chen  <https://orcid.org/0000-0001-5031-3871>

Jan D. Huizinga  <https://orcid.org/0000-0001-8016-1055>

## REFERENCES

- Rodriguez L, Sood M, Di Lorenzo C, Saps M. An ANMS-NASPGHAN consensus document on anorectal and colonic manometry in children. *Neurogastroenterol Motil.* 2019;29(1):e12944.
- Camilleri M, Bharucha AE, Di Lorenzo C, et al. American Neurogastroenterology and Motility Society consensus statement on intraluminal measurement of gastrointestinal and colonic motility in clinical practice. *Neurogastroenterol Motil.* 2008;20(12):1269-1282.
- Giorgio V, Borrelli O, Smith VV, et al. High-resolution colonic manometry accurately predicts colonic neuromuscular pathological phenotype in pediatric slow transit constipation. *Neurogastroenterol Motil.* 2013;25(1):70-e9.
- Dinning PG, Wiklendt L, Maslen L, et al. Colonic motor abnormalities in slow transit constipation defined by high resolution, fibre-optic manometry. *Neurogastroenterol Motil.* 2015;27:379-388.
- Rao SSC, Sadeghi P, Beatty J, Kavlock R, Ackerson K. Ambulatory 24-h colonic manometry in healthy humans. *Am J Physiol Gastrointest Liver Physiol.* 2001;280(4):G629-G639.
- Chen J-H, Parsons SP, Shokrollahi M, et al. Characterization of simultaneous pressure waves as biomarkers for colonic motility assessed by high-resolution colonic manometry. *Front Physiol Gastrointestinal Sci.* 2018;9:1248.
- Corsetti M, Pagliaro G, Demedts I, et al. Pan-colonic pressurizations associated with relaxation of the anal sphincter in health and disease: a new colonic motor pattern identified using high-resolution manometry. *Am J Gastroenterol.* 2017;112:479-489.
- Lin AY, Du P, Dinning PG, et al. High-resolution anatomic correlation of cyclic motor patterns in the human colon: evidence of a rectosigmoid brake. *Am J Physiol Gastrointest Liver Physiol.* 2017;312(5):G508-G515.
- Rao SS, Sadeghi P, Batterson K, et al. Altered periodic rectal motor activity: a mechanism for slow transit constipation. *Neurogastroenterol Motil.* 2001;13(6):591-598.
- Snape WJ Jr, Carlson GM, Matarazzo SA, et al. Evidence that abnormal myoelectrical activity produces colonic motor dysfunction in the irritable bowel syndrome. *Gastroenterology.* 1977;72(3):383-387.
- Narducci F, Bassotti G, Gaburri M, Morelli A. Twenty four hour manometric recording of colonic motor activity in healthy man. *Gut.* 1987;28(1):17-25.
- Rao SS, Welcher K. Periodic rectal motor activity: the intrinsic colonic gatekeeper. *Am J Gastroenterol.* 1996;91(5):890-897.
- Dinning PG, Wiklendt L, Maslen L, et al. Quantification of in vivo colonic motor patterns in healthy humans before and after a meal revealed by high-resolution fiber-optic manometry. *Neurogastroenterol Motil.* 2014;26(10):1443-1457.
- Sarna SK, Waterfall WE, Bardakjian BL, Lind JF. Types of human colonic electrical activities recorded postoperatively. *Gastroenterology.* 1981;81(1):61-70.
- Bueno L, Fioramonti J, Ruckebusch Y, Frexinos J, Coulom P. Evaluation of colonic myoelectrical activity in health and functional disorders. *Gut.* 1980;21(6):480-485.
- Huizinga JD, Waterfall WE. Electrical correlate of circumferential contractions in human colonic circular muscle. *Gut.* 1988;29(1):10-16.
- Huizinga JD. The physiology and pathophysiology of interstitial cells of Cajal: pacemaking, innervation, and stretch sensation. In Said H, Kaunitz JK, Ghishan F, Merchant J, Wood J (Eds.), *Physiology of the Gastrointestinal Tract.* Elsevier; 2018: 305-336.
- Blair PJ, Rhee P-L, Sanders KM, Ward SM. The significance of interstitial cells in neurogastroenterology. *J Neurogastroenterol Motil.* 2014;20(3):294-317.
- Huizinga JD, Lammers WJ. Gut peristalsis is governed by a multitude of cooperating mechanisms. *Am J Physiol Gastrointest Liver Physiol.* 2009;296(1):G1-G8.
- Knowles CH, Farrugia G. Gastrointestinal neuromuscular pathology in chronic constipation. *Best Pract Res Clin Gastroenterol.* 2011;25(1):43-57.
- Hasler WL. Is constipation caused by a loss of colonic interstitial cells of Cajal? *Gastroenterology.* 2003;125(1):264-265.
- Der-Silaphet T, Malysz J, Hagel S, Arsenault AL, Huizinga JD. Interstitial cells of Cajal direct normal propulsive contractile activity in the mouse small intestine. *Gastroenterology.* 1998;114(4):724-736.
- Farrugia G. Reply to: Hasler, WL. Is constipation caused by a loss of colonic interstitial cells of Cajal? *Gastroenterology* 125 (2003) 264-265. *Gastroenterology.* 2003;125:265-266.
- Cipriani G, Gibbons SJ, Verhulst PJ, et al. Diabetic Csf1 op/op-mice lacking macrophages are protected against the development of delayed gastric emptying. *Cell Mol Gastroenterol Hepatol.* 2016;2(1):40-47.
- Coss-Adame E, Rao SSC, Valestin J, Ali-Azamar A, Remes-Troche JM. Accuracy and reproducibility of high-definition anorectal manometry and pressure topography analyses in healthy subjects. *Clin Gastroenterol Hepatol.* 2015;13(6):1143-1150. e1.
- Liem O, Burgers RE, Connor FL, et al. Solid-state vs water-perfused catheters to measure colonic high-amplitude propagating contractions. *Neurogastroenterol Motil.* 2012;24(4):345-e167. <https://doi.org/10.1111/j.1365>.
- Koppen IJN, Wiklendt L, Yacob D, Di Lorenzo C, Benninga MA, Dinning PG. Motility of the left colon in children and adolescents with functional constipation; a retrospective comparison between solid-state and water-perfused colonic manometry. *Neurogastroenterol Motil.* 2018;30(9):e13401.
- Chen J-H, Yu Y, Yang Z, et al. Intraluminal pressure patterns in the human colon assessed by high-resolution manometry. *Sci Rep.* 2017;7:41436.
- Rao SSC, Sadeghi P, Beatty J, Kavlock R. Ambulatory 24-hour colonic manometry in slow-transit constipation. *Am J Gastroenterol.* 2004;99(12):2405-2416.
- Vather R, O'Grady G, Lin AY, et al. Hyperactive cyclic motor activity in the distal colon after colonic surgery as defined by high-resolution colonic manometry. *Br J Surg.* 2018;105(7):907-917.
- Wiklendt L, Mohammed SD, Scott SM, Dinning PG. Classification of normal and abnormal colonic motility based on cross-correlations of pancolonic manometry data. *Neurogastroenterol Motil.* 2013;25(3):e215-e223.
- Huizinga JD, Chen J-H, Fang Zhu Y, et al. The origin of segmentation motor activity in the intestine. *Nat Commun.* 2014;5:3326.
- Code CF, Hightower NC Jr, Morlock CG. Motility of the alimentary canal in man; review of recent studies. *Am J Med.* 1952;13(3):328-351.
- Kerlin P, Zinsmeister A, Phillips S. Motor responses to food of the ileum, proximal colon, and distal colon of healthy humans. *Gastroenterology.* 1983;84(4):762-770.
- Bampton PA, Dinning PG, Kennedy ML, Lubowski DZ, Cook IJ. The proximal colonic motor response to rectal mechanical and chemical stimulation. *Am J Physiol Gastrointest Liver Physiol.* 2002;282(3):G443-G449.
- Bampton PA, Dinning PG, Kennedy ML, Lubowski DZ, deCarle D, Cook IJ. Spatial and temporal organization of pressure patterns throughout the unprepared colon during spontaneous defecation. *Am J Gastroenterol.* 2000;95(4):1027-1035.
- Cook IJ, Furukawa Y, Panagopoulos V, Collins PJ, Dent J. Relationships between spatial patterns of colonic pressure and individual movements of content. *Am J Physiol Gastrointest Liver Physiol.* 2000;278(2):G329-G341.
- Vather R, O'Grady G, Arkwright JW, et al. Restoration of normal colonic motor patterns and meal responses after distal colorectal resection. *Br J Surg.* 2016;103(4):451-461.

39. Couturier D, Roze C, Couturier-Turpin MH, Debray C.: Electromyography of the colon in situ. An experimental study in man and in the rabbit. *Gastroenterology*. 1969;56(2):317-322.
40. Schang JC, Devroede G. Fasting and postprandial myoelectric spiking activity in the human sigmoid colon. *Gastroenterology*. 1983;85(5):1048-1053.
41. Huizinga JD, Stern HS, Chow E, Diamant NE, El-Sharkawy TY. Electrophysiologic control of motility in the human colon. *Gastroenterology*. 1985;88(2):500-511.
42. Huizinga JD, Stern HS, Chow E, Diamant NE, El-Sharkawy TY. Electrical basis of excitation and inhibition of human colonic smooth muscle. *Gastroenterology*. 1986;90(5 Pt 1):1197-1204.
43. Rumessen JJ, Vanderwinden J-M, Rasmussen H, Hansen A, Horn T. Ultrastructure of interstitial cells of Cajal in myenteric plexus of human colon. *Cell Tissue Res*. 2009;337(2):197-212.
44. Rumessen JJ, Thuneberg L. Pacemaker cells in the gastrointestinal tract: interstitial cells of Cajal. *Scand J Gastroenterol Suppl*. 1996;216:82-94.
45. Christensen J. Myoelectric control of the colon. *Gastroenterology*. 1975;68(3):601-609.
46. Huizinga JD, Parsons SP. Pacemaker network properties determine intestinal motor pattern behaviour. *Exp Physiol*. 2019;104:623-624.
47. Parsons SP, Huizinga JD. Phase waves and trigger waves: emergent properties of oscillating and excitable networks in the gut. *J Physiol*. 2018;596:4819-4829.
48. Parsons SP, Huizinga JD. The phase response and state space of slow wave contractions in the small intestine. *Exp Physiol*. 2017;102(9):1118-1132.
49. Wei R, Parsons SP, Huizinga JD. Network properties of ICC affect intestinal pacemaker activities and motor patterns, according to a mathematical model of weakly coupled oscillators. *Exp Physiol*. 2017;102:329-346.
50. Quan X, Yang Z, Xue M, Chen J-H, Huizinga JD. Relationships between motor patterns and intraluminal pressure in the 3-taeniated proximal colon of the rabbit. *Sci Rep*. 2017;7:42293.
51. Picon L, Lémann M, Flourié B, Rambaud J-C, Rain J-D, Jian R. Right and left colonic transit after eating assessed by a dual isotopic technique in healthy humans. *Gastroenterology*. 1992;103(1):80-85.
52. Ritchie JA. Colonic motor activity and bowel function. I. Normal movement of contents. *Gut*. 1968;9(4):442-456.
53. Dinning PG, Sia TC, Kumar R, et al. High-resolution colonic motility recordings in vivo compared with ex vivo recordings after colectomy, in patients with slow transit constipation. *Neurogastroenterol Motil*. 2016;28:1824-1835.
54. Bassotti G, Chiarioni G, Germani U, Battaglia E, Vantini I, Morelli A. Endoluminal instillation of bisacodyl in patients with severe (slow transit type) constipation is useful to test residual colonic propulsive activity. *Digestion*. 1999;60(1):69-73.
55. Bassotti G, Battaglia E, de Roberto G, Morelli A, Tonini M, Villanacci V. Alterations in colonic motility and relationship to pain in colonic diverticulosis. *Clin Gastroenterol Hepatol*. 2005;3:248-253.
56. Moreno-Osset E, Bazzocchi G, Lo S, et al. Association between postprandial changes in colonic intraluminal pressure and transit. *Gastroenterology*. 1989;96(5 Pt 1):1265-1273.
57. Bampton PA, Dinning PG, Kennedy ML, et al. Prolonged multi-point recording of colonic manometry in the unprepared human colon: providing insight into potentially relevant pressure wave parameters. *Am J Gastroenterol*. 2001;96(6):1838-1848.
58. Dinning PG, Benninga MA, Southwell BR, et al. Paediatric and adult colonic manometry: a tool to help unravel the pathophysiology of constipation. *World J Gastroenterol*. 2010;16(41):5162-5172.
59. Bassotti G, Chistolini F, Battaglia E, et al. Are colonic regular contractile frequency patterns in slow transit constipation a relevant pathophysiological phenomenon. *Dig Liver Dis*. 2003;35(8):552-556.
60. Parsons SP, Huizinga JD. Spatial noise in coupling strength and natural frequency within a pacemaker network: consequences for development of intestinal motor patterns according to a weakly coupled oscillator model. *Front Neurosci*. 2016;10:19.

## SUPPORTING INFORMATION

Additional supporting information may be found online in the Supporting Information section.

**How to cite this article:** Pervez M, Ratcliffe E, Parsons SP, Chen J-H, Huizinga JD. The cyclic motor patterns in the human colon. *Neurogastroenterol Motil*. 2020;32:e13807. <https://doi.org/10.1111/nmo.13807>